

Review

Metal ion recognition in aqueous solution by highly preorganized non-macrocyclic ligands[☆]

Robert D. Hancock^{*}, Darren L. Melton, James M. Harrington, F. Crisp McDonald,
Raymond T. Gephart, Lindsay L. Boone, S. Bart Jones, Nolan E. Dean,
Jason R. Whitehead, Gregory M. Cockrell

Department of Chemistry and Biochemistry, University of North Carolina Wilmington, Wilmington, NC 28403, USA

Received 8 September 2006; accepted 23 October 2006

Available online 28 October 2006

Contents

1. Introduction	1678
Acknowledgment	1688
References	1688

Abstract

The metal ion complexing properties of highly preorganized non-macrocyclic ligands in aqueous solution are discussed and contrasted with those of less preorganized analogues that have simple ethylene bridges between the donor atoms. High levels of preorganization can be achieved using cyclohexenyl bridges between ligand donor atoms, use of reinforced bridges such as bispindines, or by use of extended aromatic systems as bridges, such as those found in 1,10-phenanthroline (1,10-phen). Cyclohexenyl groups increase thermodynamic stability of metal ion complexes, as indicated by $\log K_1$ values (formation constants), that increase by between 1 and 5 log units compared to less preorganized analogues. The way in which such bridges alter selectivity in the direction of smaller metal ions is discussed. Rigid bridges such as those provided by bispindine are discussed in terms of increased $\log K_1$ values, and sharply increased selectivity for smaller metal ions. Ligands derived from 1,10-phen by placing donor groups at the 2- and 9-positions are discussed, including examples with acetates (PDA), pyridyls (DPP) and phenolates (DHP). The five-membered chelate rings of PDA lead to strong selectivity for larger metal ions, including Cd(II), La(III), and Gd(III). Possible uses of PDA type ligands for Gd(III)-based MRI agents are discussed. The remarkably high stability of complexes of PDA is discussed in terms of the role of H-bonding with the solvent in stabilizing complexes with metal ions, and the very high level of preorganization of the ligand.

© 2006 Elsevier B.V. All rights reserved.

Keywords: Metal ions; Ligands; Ligand design; Preorganization; MRI; Gadolinium; Metal ion recognition; Formation constants; Biomedical applications

1. Introduction

Ligand design is important in biomedical [1], biological [2], and environmental [3] applications, and in metal ion separations [4], in which ligand preorganization [5] has been of importance. Ligands such as crown ethers [6] and cryptands [7] owe the higher thermodynamic stability of their complexes, and their sharper metal ion selectivity, to high levels of ligand preorganization [8–10]. A ligand is more preorganized the more nearly

it is constrained as the free ligand to be in the conformation required to complex the target metal ion [5]. Selectivity for one metal ion over another is measured as the difference in $\log K_1$ (the formation constant) between the two metal ions with the particular ligand.

The cyclic structure of macrocyclic ligands leads to lengthier syntheses, and considerably greater expense, than for non-macrocyclic analogs. This may have contributed to lesser commercial use of macrocycles than might have been anticipated from their interesting metal ion complexing properties. A reviewer has also suggested that slow rates of metallation have been detrimental in many potential applications. Highly preorganized non-macrocyclic ligands might present a way forward in applications of ligands in metal ion complexation. Perhaps

[☆] Based on a keynote lecture presented at the 37th International Conference on Coordination Chemistry, 13–18 August 2006, Cape Town, South Africa.

^{*} Corresponding author. Tel.: +1 910 962 3025; fax: +1 910 962 3013.

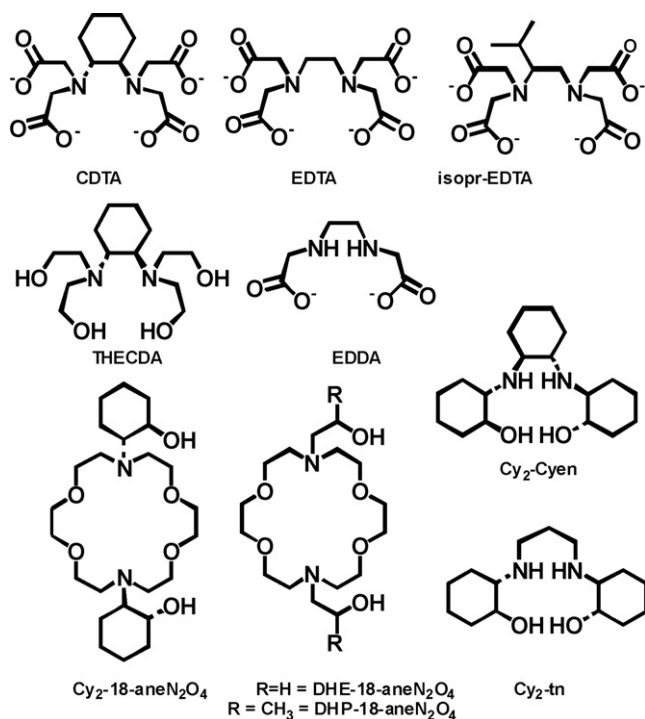


Fig. 1. Structures of ligands discussed in the first part of this review.

the earliest example of a high level of preorganization in a non-macrocyclic poly dentate ligand dates back to CDTA (see Fig. 1 for key to ligand abbreviations in the first part of this paper) studied by Schwarzenbach et al. [11]. In contrast to EDTA, the *trans*-cyclohexylene bridge between the two N-donors of CDTA constrains the N-donors to be in the *gauche* conformation required for complexing the metal ion, whereas EDTA itself should prefer the anti conformation for the ethylene bridge between the two N-donors. This has the effect that the $\log K_1$ values [12] for metal ions with CDTA are several log units higher than for the corresponding EDTA complexes. CDTA shows some important indications of high levels of preorganization [13], in that (1) there is, as mentioned above, considerable thermodynamic stabilization of the complexes of CDTA compared to its less preorganized analogue, EDTA; (2) CDTA shows sharper metal ion selectivity, which, as discussed below, is based on metal ion size; (3) rates of metallation and demetallation of CDTA complexes are slower than for EDTA, so that there is a kinetic effect of the higher levels of preorganization of CDTA. These are features of preorganization also found in macrocyclic ligands [6–8], although it should be pointed out that the popular idea of ‘size-match selectivity’ is an oversimplification of the factors that control selectivity of macrocycles for metal ions [8]. By size-match selectivity is meant the idea that macrocycles have a cavity of fairly fixed dimensions that complexes best with a metal ion whose radius corresponds with that of the cavity.

The metal ion size-based selectivity of CDTA compared to EDTA is at first sight a little surprising [13], as discussed below. It is found that the cyclohexylene bridge of CDTA shifts selectivity in the direction of smaller metal ions. The metal-ion size-related change in $\log K_1$ in passing from EDTA to CDTA

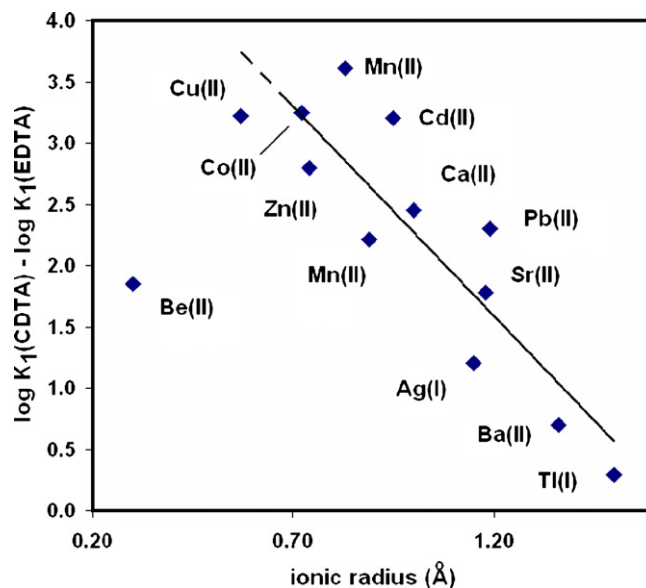


Fig. 2. Change in $\log K_1$ ($\Delta \log K_1$) in passing from EDTA to CDTA, as a function of metal-ion radius [14] (r^+). The line drawn is a least-squares best-fit relationship, $\Delta \log K_1 = -3.43(r^+) + 5.69$, with a correlation coefficient (R) = 0.884. In fitting the line, the point for Be(II) was excluded, as discussed in the text. $\log K_1$ values are from ref. [12].

for divalent and univalent metal ions is shown in Fig. 2. This is a type of diagram [8] that allows for statistical analysis of the significance of the correlation between change in $\log K_1$ and the ionic radii [14] of the metal ions. A least-squares best-fit line has been fitted to the data in Fig. 2, which has a correlation coefficient (R) of 0.884. In fitting the line, the point for Be(II) was excluded. Possibly the coordination number of 4 typically found [15] for Be(II) means that it does not follow the $\log K_1$ patterns with the hexadentate EDTA and CDTA ligands expected from Fig. 2. Alternatively, there is a maximum in the relationship between $\Delta \log K_1$ and r^+ , and the position of the point for Be(II) is not an aberration. This suggestion is supported by a similar correlation for trivalent metal ions. These points are not included in Fig. 2 because they are offset from the points for the divalent metal ions, but very small trivalent metal ions such as Al(III) and Co(III) also show smaller increases in $\log K_1$ in passing from EDTA to CDTA as compared to larger M(III) ions.

The effect of cyclohexylene bridges is generally to shift selectivity in the direction of smaller metal ions compared to analogues with ethylene bridges. For a variety of ligands with cyclohexylene bridges, ranging from the macrocycle Cy₂-18-ane-N₂O₄ to the highly preorganized Cy₂-Cyen, selectivity is shifted in the direction of small metal ions. This is illustrated in Fig. 3 for Cy₂-18-ane-N₂O₄ compared to DHE-18-ane N₂O₄. One sees that, as with CDTA and EDTA in Fig. 2, the cyclohexylene bridges in Cy₂-18-ane-N₂O₄ shift selectivity towards smaller metal ions, as compared to DFtP-18-ane-N₂O₄.

It was stated above that it might be a little surprising that the presence of cyclohexenyl bridges shifts selectivity in the direction of smaller metal ions as compared with analogues with ethylene bridges. This is because the chelate ring formed whether there is a cyclohexenyl bridge, or an ethylene bridge,

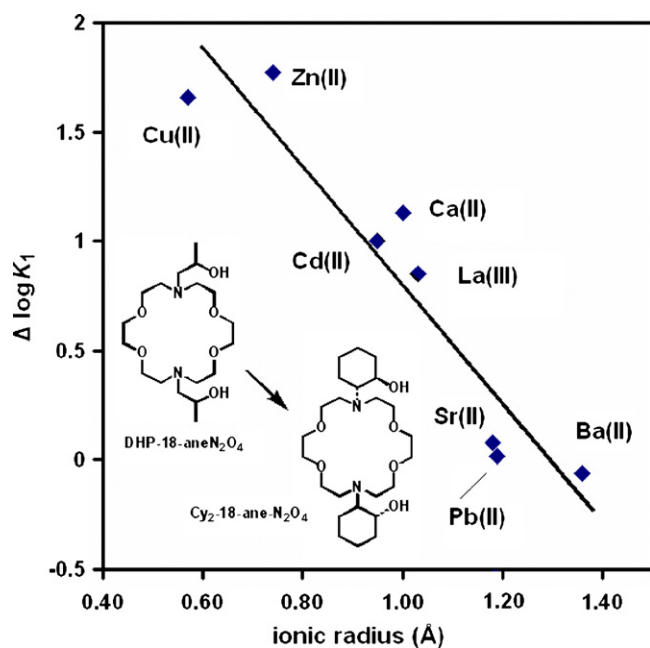


Fig. 3. Relationship between $\Delta \log K_1$ the change in $\log K_1$ in passing from the BHE-18-ane- N_2O_4 to the Cy_2 -18-ane- N_2O_4 complexes of metal ions, vs. the ionic radii [14] of the metal ions. The relationship shows that the cyclohexenyl bridge of Cy_2 -18-ane- N_2O_4 shifts selectivity in the direction of smaller metal ions, compared to the ethylene bridge of DHP-18-ane- N_2O_4 . $\log K_1$ data from ref. [12].

is a five-membered chelate ring, and it has been stated [8] that five-membered chelate rings favor larger metal ions, while six-membered chelate rings favor smaller metal ions. The geometric basis for the latter argument is presented in Fig. 4, where the size of metal ion that fits best [8] in a chelate ring involving ethylenediamine or 1,3-propanediamine is shown, as well as for the aromatic ring systems 1,10-phen and DPN (dipyridonaphthalene):

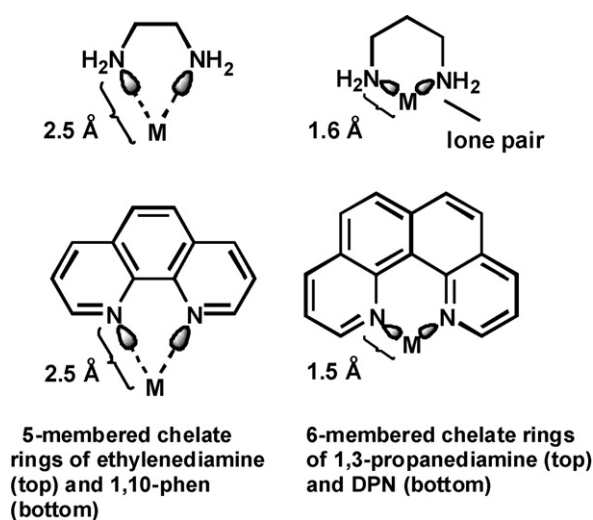


Fig. 4. Best-fit M–N lengths [8] for metal ions to form a minimum-strain chelate ring with ethylenediamine and 1,10-phen (five-membered chelate rings) or 1,3-propanediamine and DPN (dipyridonaphthalene) (six-membered chelate rings).

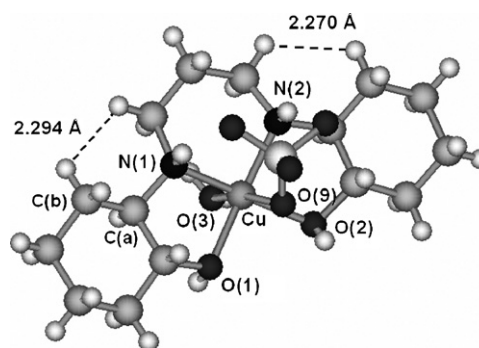


Fig. 5. Structure of the Cu(II) complex of Cy_2 -tn. The atom O(9) is from a coordinated perchlorate, while O(3) is from a coordinated water molecule. Short H–H non-bonded separations discussed in the text are indicated. In this structure the shortest contacts are between H-atoms on the ethylene bridges and H-atoms on the indicated C(b) atoms of the cyclohexylene bridges.

It should be noted that chelate ring size appears [8] to be the dominant architectural feature in controlling metal-ion size-based selectivity. It is usually more important than macrocyclic ring size for ligands such as tetraazamacrocycles [8], since macrocycles are able to assume a variety of energetically similar conformations that are able to accommodate metal ions of different sizes. It is thus perhaps surprising that the rigid five-membered chelate ring involving the cyclohexenyl bridge does not enhance affinity for large metal ions, but moves ligand selectivity in the direction of smaller metal ions. The answer to this apparent paradox is that [16] bulky groups such as the cyclohexenyl bridge produce steric crowding in the coordinated ligand, which decreases as the metal ion gets smaller and increases the curvature of the ligand. This is seen in Fig. 5, where the Cu(II) complex [17] of Cy_2 -tn is shown. The short H–H contacts, less than the sum of the van der Waals radii [18] of two non-bonded H-atoms of 2.40 Å are indicated. One can see that as the metal ion becomes larger, so the curvature of the ligand will decrease, and the H–H non-bonded contacts indicated will become shorter.

The above steric crowding effects occur with any substituents, not just cyclohexenyl groups. Thus, placing any C-alkyl substituents on EDTA, either on the ethylene bridge, or the methylenes of the acetate groups, will shift selectivity in the direction of smaller metal ions. Steric crowding effects may even be important for increase of chelate ring size in passing from ethylene bridges to trimethylene bridges as indicated in Fig. 4. The effect of addition of C-alkyl groups to ligands is seen in Fig. 6, where an isopropyl group is added to the ethylene bridge of EDTA. It is seen that, just as with CDTA and EDTA, the isopropyl group of isopr-EDTA shifts selectivity towards smaller metal ions as compared with EDTA. This type of result has led to the suggestion [16] that nearly all purely architectural changes in complex structure will produce changes in complex stability that are directly related to metal-ion radius. Where metal ions have very strong preferences for particular coordination geometries, such as the linear coordination geometry of Ag(I) and Hg(II) , or the square planar geometry of Pd(II) , this too can be important, but in an obvious and predictable way. An important aspect of the relationship between metal-ion size and selectivity is steric crowding, as with alkyl substitution of chelate rings, as seen in

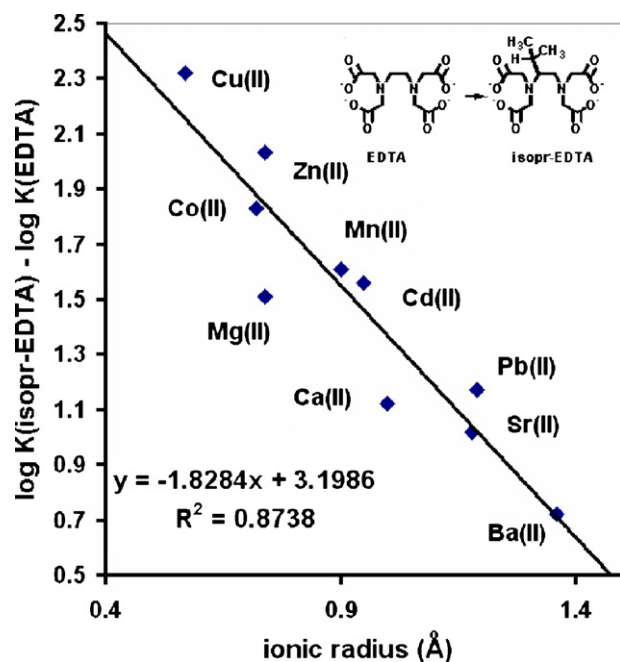


Fig. 6. Linear free energy relationship (LFER) showing metal ion size-related change in selectivity ($\Delta \log K_1$, which here is $\log K(\text{isopr-EDTA}) - \log K(\text{EDTA})$) as a function of metal ion radius for isopr-EDTA relative to EDTA. $\Delta \log K$ is $\log K$ for the equilibrium: $\text{M}(\text{EDTA}) + \text{isopr-EDTA} \rightleftharpoons \text{M}(\text{isopr-EDTA}) + \text{EDTA}$. Ionic radii [14] for octahedral metal ions except for Cu(II) which is the square planar radius.

Figs. 2, 3 and 6. Clearly, the van der Waals repulsions between substituents on ligands will be dependent on M–L length, and not respond much to the nature of the M–L bond, i.e. whether the M–L bond is covalent or ionic. This accounts for the great range of M–L bonding types obeying the correlation in Figs. 3 and 6, from very ionically bound metal ions such as Ba(II), to the more covalently bound Cu(II). Selectivity effects such as those due to chelate ring size illustrated in Fig. 2 also appear to be rather insensitive to M–L bonding type, again because what one is seeing is dependent largely only on M–L bond length.

A reviewer has suggested that the possibility has been ignored that the trends in Figs. 2, 3 and 6, and also the effects explained sterically in Fig. 4, could be explained in terms of inductive effects. The present corresponding author is certainly not unaware of the importance of inductive effects [19–24], and was the first to point out the role of inductive effects as N-donors are changed along the series $1^\circ < 2^\circ < 3^\circ$ in producing high ligand field (LF) strengths and higher thermodynamic stability in complexes of tetraazamacrocycles [20] compared to their open-chain analogues. Particularly important here is the first observation of the role of *N*-alkyl substituents along the series methyl < ethyl < isopropyl < *t*-butyl in raising $\log K_1$ for large metal ions of low coordination number such as Ag(I) [19] or Pb(II) [22]. What seem best explained as pure inductive effects, particularly as appear to occur for the linear Ag(I) complexes, where steric effects would be minimal, along the series methylamine, ethylamine, isopropylamine, and *t*-butylamine, produce only small increases [19] in $\log K_1$. It has already been suggested that inductive effects may contribute [8,20,24], along with the

accompanying, increased preorganization of the ligand [23,24], to increases in complex stability seen in Figs. 2, 3 and 6. Inductive effects do not appear to be the major contribution to the observed metal-ion selectivity patterns evident in Figs. 2, 3, or 6. This is seen in that where C-alkyl groups are added to ligands where steric crowding will not occur, no metal-ion size-related change in selectivity is observed. Thus, for any ligand of high denticity, replacing ethylene bridges with cyclohexenyl bridges, or adding C-alkyl substituents to ethylene bridges, will shift selectivity in the direction of smaller metal ions. The steric interactions that are important in addition of C-alkyl groups are those, as seen in Fig. 5 that occur between the alkyl substituent and adjacent chelate rings. Where there are no adjacent chelate rings to produce such steric crowding, no shift in selectivity towards smaller metal ions occurs on adding C-alkyl substituents. Thus, if the complexes of ethylenediamine (en) are compared with those of *trans*-1,2-diaminocyclohexane (*trans*-DAC), only a small constant increase in $\log K_1$ [12] is observed, which does not relate to metal-ion size. If inductive effects were dominant, one would expect to see a shift in selectivity towards small metal ions such as Cu(II) that have more covalent M–N bonding, and also one would not expect very small increases in $\log K_1$ as compared to the large changes in $\log K_1$ seen in Figs. 2, 3 and 6:

	Metal ion				
	Cu(II)	Ni(II)	Co(II)	Zn(II)	Cd(II)
Ionic radius (Å)	0.57	0.69	0.72	0.74	0.95
$\log K_1(\text{en})$	10.49	7.30	5.5	5.69	5.4
$\log K_1(\text{trans-DAC})$	11.09	7.80	6.37	6.37	5.80
Increase in $\log K_1$	0.60	0.50	0.87	0.68	0.40

Ionic radii from ref. [14], $\log K_1$ values from ref. [12].

Similar to the results for en and *trans*-DAC, other alkyl substituents on en such as methyl, ethyl, or isopropyl produce only very small changes in $\log K_1$ [12] with Cu(II), as compared to the large change in $\log K_1$ seen in Fig. 6. The complex stabilization on substitution of EDTA with C-alkyl groups is so much larger than for en itself because in the case of the latter, the difference in energy between the more stable anti and the less stable gauche forms is quite small. In the case of EDTA, separation of the negative charges on the acetate groups is much larger in the anti than the gauche form, and so the energy differences between these two forms of the ligand is large. Placement of C-alkyl groups on EDTA to minimize energy differences between the gauche and anti forms thus leads to large stabilizations of the complexes. In contrast, for ligands such as THEEN and THECDA, which have neutral O-donor groups in place of the acetate groups of EDTA, the increase in $\log K_1$ on increase of preorganization by addition of cyclohexenyl bridges is quite small, as seen in Fig. 7.

A different approach to more preorganized non-macrocyclic ligands has involved reinforcement of the ligand using doubly bridged chelate rings. This approach is typified, for example, by ligands based on DACO (diazacyclooctane), such as DACODA [25–28], BME-DACO [29], or BAE-DACO [28] shown in Fig. 8. The DACO architecture has also been incorporated into N-donor macrocyclic ligands [30]. What is found with the DACO type of

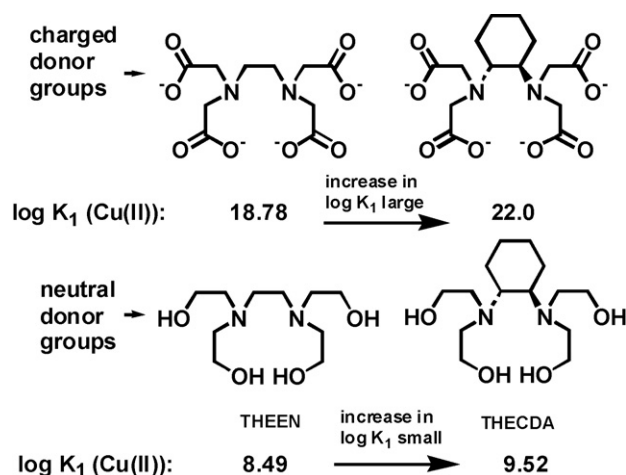


Fig. 7. Effect on $\log K_1$ [12] for Cu(II) complexes of increase in levels of ligand preorganization by (a) addition of a cyclohexenyl bridge to EDTA, which has charged acetate O-donors, and (b) THEEN, which has neutral O-donors.

bridge is that these do not produce any stabilization compared with singly bridged analogs [28], as seen in comparing $\log K_1$ values for BAE-DAC complexes, which are generally lower than for the singly bridged analog 2,3,2-tet. This arises because of the steric problems [28] associated with metal ions coordinating to double bridges such as that of BME-DACO. Thus, once coordinated to a metal ion, the DACO ring appears to assume two conformations, either the chair–chair, or the chair–boat conformation. Of the thirty structures reported in the CSD [31] for BME-DACO and related ligand complexes of low-spin Ni(II), for example, all but two [32,33] have the chair–boat conformation. This agrees with PM3 semi-empirical calculations that can be carried out with a program such as HyperChem [34], which show that for the low-spin Ni(II) complex of BME-DACO, the chair–boat conformation is some 4.4 kcal mol^{−1} lower in energy than the chair–chair conformation. Since the two struc-

tures where a chair–chair conformer might be present have the DACO rings disordered [31,32], it seems possible that these actually have superimposed chair–boat conformations, and that in fact chair–chair conformations are too high in energy to exist. Even the chair–boat conformer of the DACO chelate ring is high in energy, since this involves a high-energy boat conformation for one part of the DACO moiety, leading to no stabilization relative to analogues such as 2,3,2-tet.

The high energy of the chair–chair conformation of the DACO ring in complexes of ligands such as BAE-DACO or BME-DACO derives from a steric interaction [28] between H-atoms on the central C-atoms of the trimethylene bridges of the DACO ring (Fig. 8). One way to overcome such H–H non-bonded repulsions is to replace the H–H repulsion with covalent C–C bonds. This leads to bispidine-based bridges instead of DACO type chelate rings [35–41], as seen in Fig. 9. Bispidine is an extremely rigid molecule, particularly when a metal ion of the right size is chelated between the two N-donors. With a metal ion in position, the bispidine-based chelate ring resembles the diamond-like hydrocarbon adamantane. Complexes of bispidines have shown interesting catalytic properties [41], and N-donor macrocycles based on bispidine, first proposed some time ago [23,24], have been synthesized [42,43]. Interestingly, metallation of such macrocycles, even with the very labile Cu²⁺ ion, was so slow [42,43] as to be achieved only with great difficulty, showing that one can have too much preorganization if the aim is the sequestration of metal ions in solution. In line with predictions about the high position of 3° N-donors in the spectrochemical series when in a stereochemically efficient environment [20,23,24], the ligand field splitting of the Cu(II) complexes of macrocycles such as macrocycle 1 in Fig. 9 is remarkably high [42,43]. This is in line with the prediction [8,20] that four 3° N-donors in a sterically efficient setting will lead to very high LF splitting as compared to analogues with 2° or 1° N-donors.

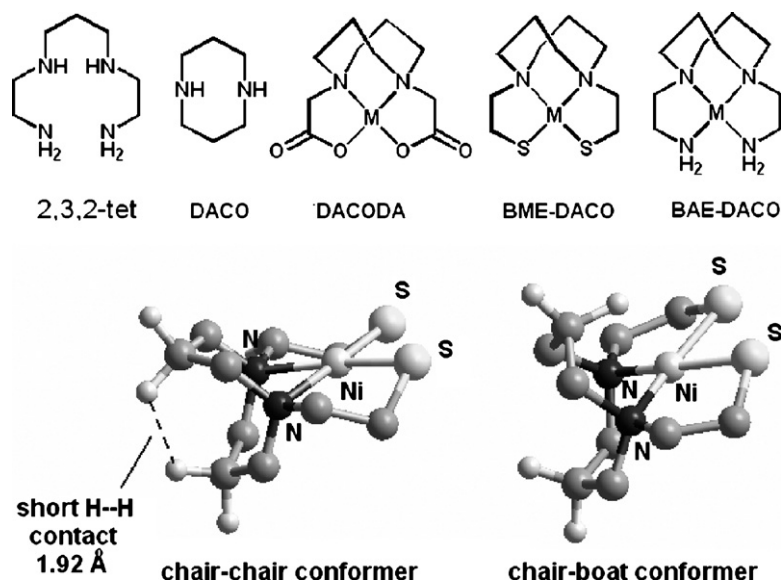


Fig. 8. Ligands based on the DACO ring [25–28], showing (below) the chair–chair and chair–boat conformers of the low-spin Ni(II) complex of BME-DACO generated by MM calculation [34]. H-atoms omitted for clarity, except for those on the central methylene groups of the trimethylene bridges between the N-donors.

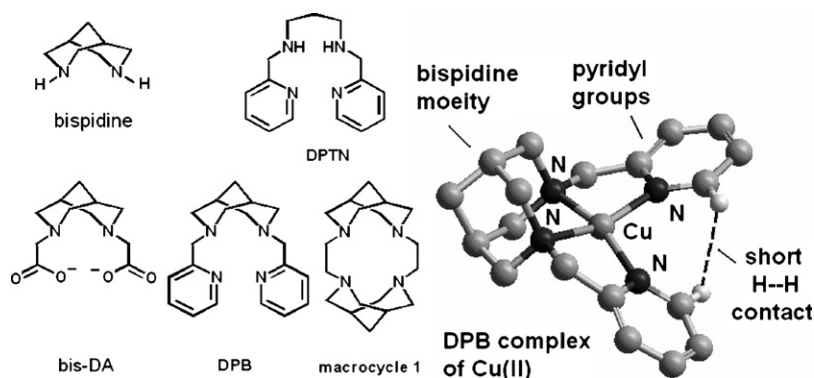


Fig. 9. Bispidine-containing ligands bis-DA [35], DPB [36] and macrocycle 1 [42], and the Cu(II) complex of DPB [36].

There is an early report of the synthesis of bispidine-*N,N'*-diacetate (bis-DA, Fig. 9), and of some complexes with a variety of metal ions [35]. The ligand DPB (Fig. 9) shows the expected effects of its highly preorganized structure [36]. The six-membered chelate ring formed by the bispidine moiety complexes well with the small H^+ and Cu^{2+} ions, and so the $\text{p}K$ value, and $\log K_1(\text{Cu}^{2+})$ are much higher than for its analog DPTN (Table 1). For larger metal ions such as $\text{Cd}(\text{II})$, the stabilization of the DPB relative to the DPTN complex is much smaller, as would be expected from the fact that DPB forms an extremely rigid six-membered chelate ring on complex-formation. Since six-membered chelate rings disfavor larger metal ions [8], one would expect a small stabilization of the DPB complex for larger metal ions, as is seen in Table 1. DPB is an interesting ligand, but suffers from the steric crowding problems associated with pyridyl groups. With pyridyl donors, H-atoms of the pyridyl ring frequently interact sterically with each other, and with other parts of the complex, thus destabilizing the complexes. One sees for the $\text{Cu}(\text{II})$ complex of DPB in Fig. 9, that the *ortho* H-atoms of the pyridyl groups prevent planar coordination to the $\text{Cu}(\text{II})$, which thus has its preferred planar coordination distorted towards tetrahedral. This distortion doubtless destabilizes the complex somewhat, and elimination of such steric effects would lead to superior ligands.

The ligand bipy presents a classic example of the steric problems caused by the H-atoms on pyridyl groups. To achieve planar coordination of the two pyridyl groups in the *cis* conformation so as to produce optimum overlap of the donor orbitals of the N-donors, and the orbitals of the metal ion, requires that the H-atoms in the 3-position on each pyridyl group come into short ($\sim 2.02 \text{ \AA}$) contact. In line with the suggestion above [16] that

most effects on metal ion selectivity due to changes in ligand architecture relate to metal-ion size, it is found that the structures of complexes of metal ions also tend to vary systematically with metal-ion size, as would be required from the above suggestion. Thus, if one examines the structures of bipy complexes found in the CSD [31], it is found that the variation of the N–M–N angle of the bipy chelate ring is directly related to the M–N length, as seen in Fig. 10(a). One might expect that if the N–N bite distance for bipy complexes was fixed at a value of 2.50 \AA suggested from molecular mechanics (MM) calculations [34] on the free ligand, then there would be, from simple geometric considerations, a relationship between M–N length and N–M–N angle as seen in Fig. 10(a).

The relationship in Fig. 10(a) shows that only with smaller metal ions with $\text{M–N} \sim 1.9 \text{ \AA}$ does bipy approach the ideal N–N bite size of 2.50 \AA . At longer M–N bond lengths there is distortion of the bipy ligand, with N–N bite distances being opened up to as much as 2.9 \AA . The steric situation with bipy is quite complex, since there are other important factors such as distortion of the M–N–C and N–C–C bond angles at short M–N lengths, that affect complex stability. Thus, in Fig. 10(b), one sees that the M–N–C angle in the bipy complexes also varies as a function of M–N length, but now is much smaller than the ideal value of 120° with small metal ions. At larger bite sizes the H–H repulsions at the 3-positions increase, so that bipy resembles ligands with cyclohexenyl bridges in that there is steric crowding on the outside of the coordinated ligand, which is worse for larger metal ions. A referee has queried how the N–C–C–N torsion angle might vary with M–N length in bipy complexes. The N–C–C–N torsion angle shows little systematic variation with M–N length. The H–H van der waals repulsion between the H-atoms in the 3- and 3'-positions of bipy is reduced as the N–C–C–N torsion angle increases. However, this benefit is offset by increasing energy as the N–C–C–N torsion angle increases, due to diminished delocalization. The trade-off between decreased H–H repulsion and higher energy as the N–C–C–N torsion angle increases appears to lead to a range where about 90% of N–C–C–N torsion angles fall between 0° and 15° . As might be expected, the few very large N–C–C–N angles appear to be associated largely with very long M–N bond lengths. The ligand 1,10-phen represents a more preorganized version of bipy, with the H–H repulsions of the H-atoms in the 3-position of

Table 1
Formation and protonation constants of DPB [36] and its non-reinforced analogue DPTN [12]^a

Lewis acid	H^+	$\text{Cu}(\text{II})$	$\text{Ni}(\text{II})$	$\text{Zn}(\text{II})$	$\text{Cd}(\text{II})$	$\text{Pb}(\text{II})$
Ionic radius (\AA) ^b	—	0.57	0.69	0.74	0.95	1.19
$\log K_1$, DPB	13.1	23.0	15.8	12.0	11.3	nec ^c
$\log K_1$, DPTN	8.33	18.35	14.2	10.33	8.48	6.4

^a See Fig. 9 for key to ligand abbreviations.

^b Ref. [14].

^c nec = no evidence for complex.

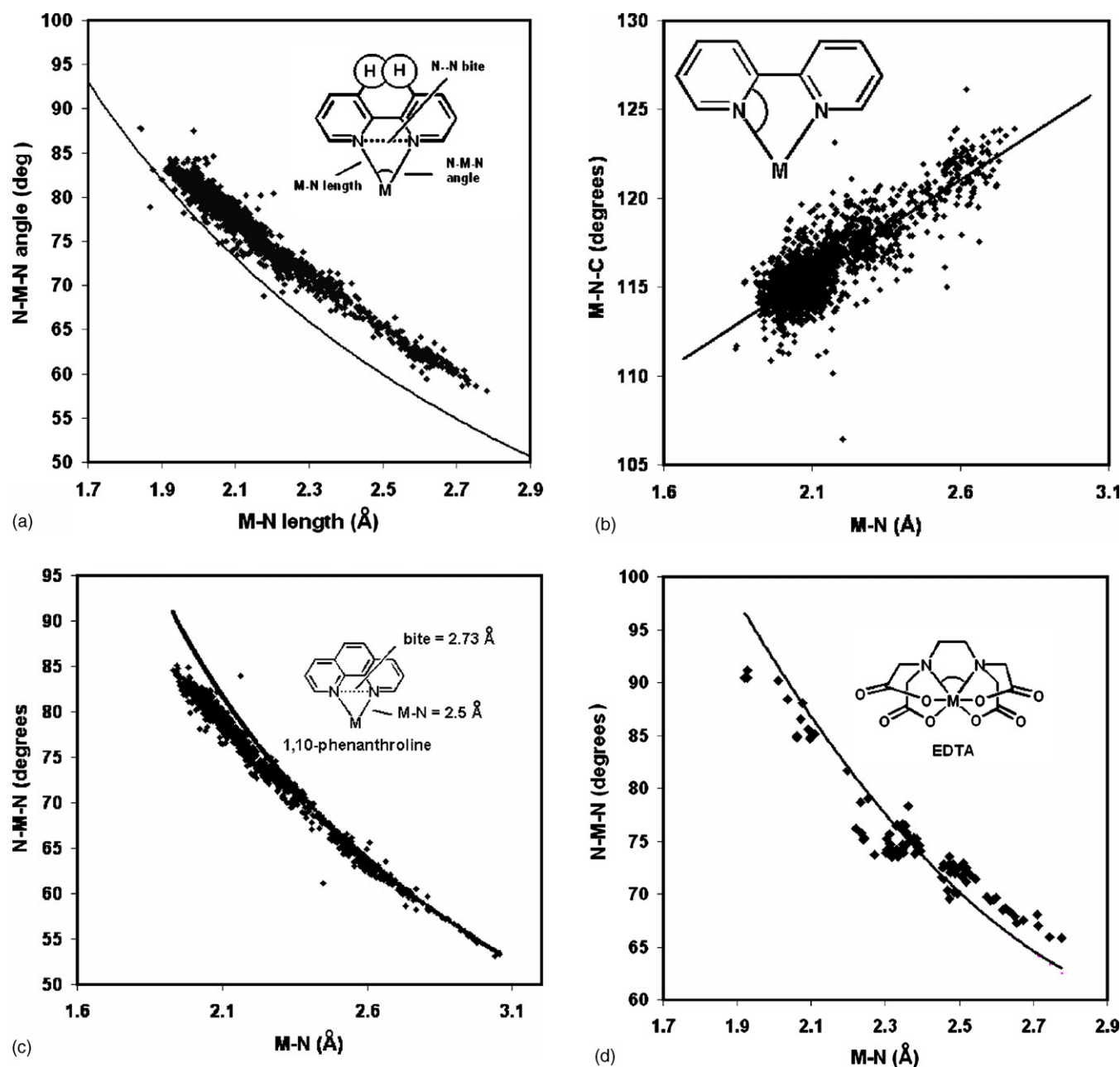


Fig. 10. (a) Relationship between N–M–N angle and M–N length for the structures of 2585 chelate rings of the bipy ligand found in the CSD [31], with $R < 0.1$. The structure drawn on the diagram shows the N–N bite distance, which MM calculation [34] suggests is 2.50 Å in the planar form of free bipy. The solid line is the theoretical curve expected for the variation of the N–M–N angle with M–N length if a fixed N–N bite distance of 2.50 Å is maintained. Also shown is the steric interaction occurring between the H-atoms on the 3- and 3'-position of bipy when in the *syn* form required for coordination to a metal ion. (b) M–N–C angles vs. M–N bond lengths for bipy complexes for 2585 chelate rings involving the bipy ligand found in the CSD [31]. The best-fit line drawn in has a correlation coefficient of 0.833. (c) Relationship between N–M–N angle and M–N length for 1330 chelate rings involving 1,10-phenanthroline (1,10-phen) as ligand with $R < 0.1$ found in the CSD [31]. The solid line is the theoretical line calculated for a fixed N–N bite distance of 2.73 Å for 1,10-phen. The N–N bite distance is the average N–N (with a standard deviation of 0.02 Å) in 35 structures containing free 1,10-phen found in the CSD with $R < 0.1$. (d) The relationship between the N–M–N angle (indicated on the diagram) in EDTA complexes, and the M–N bond length, for the structures of 101 EDTA complexes found in the CSD [31] with $R < 0.1$. The line drawn in is the theoretical relationship between the N–M–N angle and M–N length for a constant N–N bite distance of 2.88 Å. The latter bite distance is the N–N distance in the MM minimized [34] structure of ethylenediamine ligand in the gauche conformation.

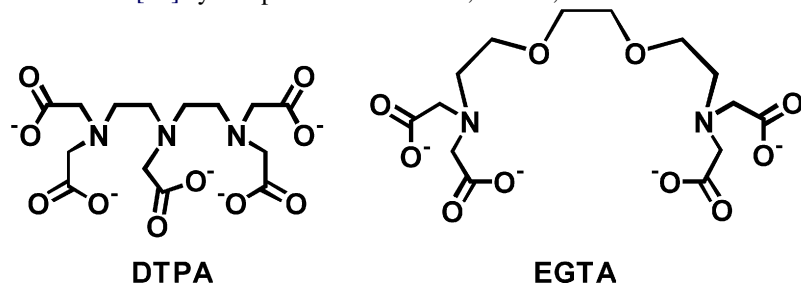
the pyridyl groups replaced with covalent C–C bonds. If one searches the CSD [31] for structures of complexes containing the 1,10-phen chelate ring, one finds a very similar relationship to that found for bipy complexes (Fig. 10(a)) between the M–N length and the N–M–N angle, as seen in Fig. 10(c). The solid line is calculated with the N–N bite distance of 2.73 Å found

from 35 structures of the free 1,10-phen ligand in the CSD [31]. One finds accordingly that $\log K_1$ values for 1,10-phen ligands are about 1.4 log units higher than for corresponding bipy complexes [8,14], with removal of the H–H repulsion problem found with bipy complexes. In Fig. 10(d) is shown the relationship between the N–M–N angle and M–N length for complexes of

EDTA. This is shown simply because the relationship is typical of those found for the structures of almost all classes of complexes [31]. The widespread occurrence of such relationships suggests why metal-ion size is so strongly related to changes in complex stability induced by changes in ligand architecture. Ligands that are found to obey relationships of the type seen in Fig. 11(a)–(d) include en, oxalate, 1,2-dimethoxyethane, 1,3-dimethoxypropane, 1,2-bis(methylthio)ethane, $R_2P(CH_2)_nPR_2$ ligands ($n = 1$ and 2), dipicolinates, acetylacetonate, catcholate, and terpyridyl complexes. What one sees is that complex structure varies in a systematic fashion with metal-ion size, as do changes in $\log K_1$ with changes in ligand structure.

Highly preorganized ligands such as 1,10-phen present ideal rigid backbones for developing highly preorganized non-macrocyclic ligands, once donor groups have been placed at the 2-position, or 2- and 9-positions. Many ligands of this type have been synthesized from 1,10-phen by substitution at the 2-, or 2- and 9-positions (Fig. 11). The driving force in the synthesis of these ligands to date has been largely for the investigation of the photochemical properties of the Ru(II) complexes [45,60,62,63,65,68], which papers are not further discussed here.

The ligand PDA best typifies the metal complexing properties of this type of ligand. One would expect the rigid 1,10-phen backbone of PDA to lead to enhanced preorganization, manifested as increased thermodynamic stability of complexes of PDA. In addition, the formation of three rigid five-membered chelate rings on complex-formation should favor larger metal ions (Fig. 4), since 1,10-phen does not have problems with steric crowding from H-atoms on its outer side that pushes selectivity somewhat towards smaller metal ions for bipy complexes. Measurement of $\log K_1$ values for PDA presents a unique problem [69], in that the complexes of virtually all metal ions with PDA are too stable to break down as the pH is lowered, which competition is the basis of most $\log K_1$ determinations with amine ligands. PDA also has poor water solubility ($\sim 10^{-4}$ M), but has very intense bands in the ultraviolet that allow for monitoring of complex-formation [70]. The $\log K_1$ values for PDA were determined [69] by competition with EDTA, DTPA, and EGTA.



In Fig. 12 is shown the variation of the spectra of 2×10^{-5} M PDA as a function of pH in 0.1 M NaClO₄. The set of spectra in (a) are for the ligand alone, the set in (b) has in addition 2×10^{-5} M Cu²⁺, and the set in (c) refers to a 1:1:1 mixture of 2×10^{-5} M of each of PDA, EDTA, and Cu²⁺. The variation of absorbance as a function of pH in (a) leads to two protonation constants. The spectra in (b) for the Cu(II)/PDA complex vary mainly as a result of dilution, showing no response to pH in the range covered, except for some changes in the pH range 2–3 that

are attributed to protonation of a non-coordinated carboxylate group. At high pH, the spectra in Fig. 12(c) are those of free PDA at that pH, showing that here the Cu(II) is bound by the EDTA. As the pH is lowered, the high pK_a values of EDTA cause the Cu(II) to be transferred to the much less basic PDA following equation:



From a knowledge of the protonation constants and formation constants for EDTA (or DTPA or EGTA) [12] one can use sets of spectra as shown in Fig. 12(c) to calculate $\log K_1$ for the metal ion with PDA. These are shown in Table 2.

PDA does not have a strictly analogous less-preorganized ligand for comparison, but EDDA (Fig. 1) is the nearest in terms of similar donor-atoms and chelate ring size. Admittedly, EDDA is a less than perfect comparison, but it should be borne in mind that in aqueous solutions saturated amines are stronger bases than pyridines [12], so that basicity differences between PDA and EDDA should favor the latter. Thus, any stabilization due to the rigid backbone of PDA should be, if anything, understated. In Table 3 the $\log K_1$ values for PDA and EDDA complexes are compared.

What Table 3 shows is that for the largest metal ions such as Pb(II) and Ba(II) ($r^+ = 1.19$ and 1.36 Å [14]), $\log K_1$ for PDA complexes is some 1–2 log units higher than for analogous EDDA complexes. For divalent metal ions such as Cd(II) and Ca(II) with ionic radii [14] close to 1.00 Å, this stabilization approaches 4 log units. For small metal ions such as Mg(II), Zn(II), and Cu(II), the EDDA complexes are more stable than the PDA complexes. This fits perfectly with MM (molecular mechanics) calculations [71] that show [69] that the best-fit size of metal ion for coordinating in the binding site of PDA has an ionic radius of 0.96 Å.

The stabilization of the PDA complexes of the trivalent La(III) and Gd(III) ions relative to EDDA is quite remarkable. These ions have radii of 1.03 and 0.96 Å, so they are close to optimum size for complexing with PDA. However, the level of

stabilization is much greater than for similarly sized divalents, so there must be additional factors operating here. One consideration is that trivalent metal ions appear to form complexes with pyridyl groups that are rather low in thermodynamic stability by comparison with saturated N-donors [72]. This is seen in Fig. 13, where $\log K_1$ for TPEN complexes [14,72,73] of M(II) and M(III) ions has been plotted against $\log K_1(NH_3)$ for the same ions. It is seen that two distinct correlations are obtained,

Table 2

The pH_{50} values^a and protonation and formation constants for a selection of metal ions with PDA [69] (0.1 M NaClO_4 , 25 °C)

Lewis acid	Equilibrium ^b	pH_{50}	$\log K_1(\text{PDA})^c$	$\log K_1(\text{PDA})_{(\text{corr})}^d$
H^+	$\text{H}^+ + \text{L}^{2-} \rightleftharpoons \text{HL}^-$	—	4.75(2)	
	$\text{H}^+ + \text{LH}^- \rightleftharpoons \text{H}_2\text{L}$	—	2.53(5)	
	$\text{H}^+ + \text{OH}^- \rightleftharpoons \text{H}_2\text{O}$	—	13.78 ^e	
Mg^{2+}	$\text{Mg}^{2+} + \text{L}^{2-} \rightleftharpoons \text{MgL}$	—	3.53(5) ^f	3.53(5)
Ca^{2+}	$\text{Ca}^{2+} + \text{L}^{2-} \rightleftharpoons \text{CaL}$	7.17(3)	8.2(1) ^g , 7.4(1) ^f	7.3(1)
	$\text{CaL} + \text{H}^+ \rightleftharpoons \text{CaLH}^+$	—	3.2(1)	3.2(1)
Sr^{2+}	$\text{Sr}^{2+} + \text{L}^{2-} \rightleftharpoons \text{SrL}$	—	5.61(4) ^f	5.61(4)
Ba^{2+}	$\text{Ba}^{2+} + \text{L}^{2-} \rightleftharpoons \text{BaL}$	—	5.43(5) ^f	5.43(5)
La^{3+}	$\text{La}^{3+} + \text{L}^{2-} \rightleftharpoons \text{LaL}^+$	8.52(4), 6.45(3) ^h	14.4(1) ^g , 15.1(1) ^h	13.5(1)
Gd^{3+}	$\text{Gd}^{3+} + \text{L}^{2-} \rightleftharpoons \text{GdL}^+$	8.08(9), 7.3(1) ^h	17.0(1) ^g , 17.6(1) ^h	16.1(1)
Zn^{2+}	$\text{Zn}^{2+} + \text{L}^{2-} \rightleftharpoons \text{ZnL}$	5.49(4)	11.9(1) ^g	11.0(1)
Cd^{2+}	$\text{Cd}^{2+} + \text{L}^{2-} \rightleftharpoons \text{CdL}$	6.67(2)	13.7(1) ^g	12.8(1)
Pb^{2+}	$\text{Pb}^{2+} + \text{L}^{2-} \rightleftharpoons \text{PbL}$	4.95(2)	12.3(1) ^g	11.4(1)
Cu^{2+}	$\text{Cu}^{2+} + \text{L}^{2-} \rightleftharpoons \text{CuL}$	5.28(4)	13.7(1) ^g	12.8(1)

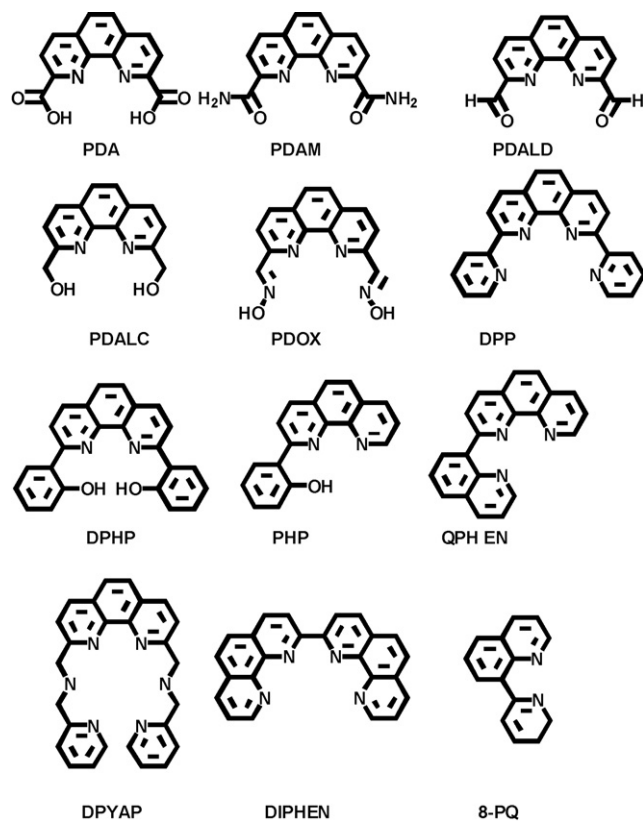
^a The pH_{50} is the pH in the equilibrium $\text{M}(\text{EDTA}) + \text{PDA} + n\text{H}^+ = \text{M}(\text{PDA}) + \text{EDTAH}_n$ at which the concentrations of $\text{M}(\text{EDTA})$ and $\text{M}(\text{PDA})$ are equal.^b In these equilibria $\text{L} = \text{PDA}$.^c Where no pH_{50} is given, these $\log K_1$ values were calculated directly from the competition between the proton and the metal ion for coordination to the ligand. Where a pH_{50} is given, $\log K_1(\text{PDA})$ was calculated from the pH_{50} and a literature value [12] for $\log K_1(\text{EDTK})$.^d These are corrected, as described in the text, for the fact that the $\log K_1(\text{EDTA})$ values used in calculating $\log K_1(\text{PDA})$ do not include competition from the Na^+ ion, which should lower $\log K_1(\text{PDA})$ by about 0.9 log units.^e From ref. [12].^f Calculated by using bands in spectrum between 200 and 350 nm to monitor the equilibrium $\text{M}(\text{PDA}) + n\text{H}^+ = \text{M} + \text{PDAH}_n$.^g Calculated from pH_{50} and the reported [12] value for $\log K_1(\text{EDTA})$ as described in the text.

Fig. 11. Highly preorganized ligands based on pyridyl donor groups mentioned in this paper. References: PDA [69,74–78], PDAM-PDOX [44], DPP [68], DPHP [48], PHP [46,47,50], QPHEN [45], DPYAP [57], DIPHEN [62,63,65], 8-PQ [60]. Other ligands of interest based on 1,10-phenanthroline with a variety of substituents in the 2 and 9 positions, not directly related to the subject matter of this review, have also been reported [49,51–59,61,64,66,67].

with $\log K_1$ for $\text{M}(\text{III})$ ions with the pyridyl-containing TPEN ligand being displaced to lower $\log K_1$ than for $\text{M}(\text{II})$ ions. The origin of the lower than expected $\log K_1$ (TPEN) values for $\text{M}(\text{III})$ ions suggested by Fig. 13 may lie in the need for ions to be stabilized by transfer of charge to the solvent by H-bonding. This would clearly be more important for $\text{M}(\text{III})$ than for $\text{M}(\text{II})$ ions, and pyridyl groups are unable to H-bond with the solvent, which may account for the lower than expected $\log K_1$ (TPEN) values for $\text{M}(\text{III})$ ions in Fig. 13. In PDA complexes, the presence of the carboxylates may act to lower the charge on the $\text{M}(\text{III})$ ions, hence removing the need for strong H-bonding with the solvent by coordinated pyridyl groups.

The very large stabilization of PDA complexes of $\text{M}(\text{III})$ ions with an ionic radius of about 1.0 Å seen in Table 3 suggests that

Table 3

Formation constants (0.1 M NaClO_4 , 25 °C) for a selection of metal ions with PDA [69] and with EDDA [12], plus ionic radii of the metal ions^a

Metal ion	Ionic radius ^b	$\log K_1(\text{PDA})^c$	$\log K_1(\text{EDDA})^d$	$\Delta \log K^e$
Ba^{2+}	1.36	5.4	3.3	2.1
Pb^{2+}	1.19	11.4	10.6	0.8
Sr^{2+}	1.18	5.6	3.6	2.0
Ca^{2+}	1.00	7.3	4.0	3.3
La^{3+}	1.03	13.5	7.0	6.5
Gd^{3+}	0.93	16.1	8.1	8.0
Cd^{2+}	0.95	12.8	9.1	3.7
Mg^{2+}	0.74	3.5	4.0	−0.5
Zn^{2+}	0.74	11.0	11.1	−0.1
Cu^{2+}	0.57	12.8	16.2	−3.4

^a Ionic strength = 0.1 M at 25 °C.^b Units = Å, ref. [14].^c Uncertainty in $\log K \sim 0.1$.^d Ref. [12], ionic strength 0.1. EDDA = ethylenediamine- N,N' -diacetate.^e $\Delta \log K$ for $\text{M}(\text{EDDA}) + \text{PDA} = \text{M}(\text{PDA}) + \text{EDDA}$.

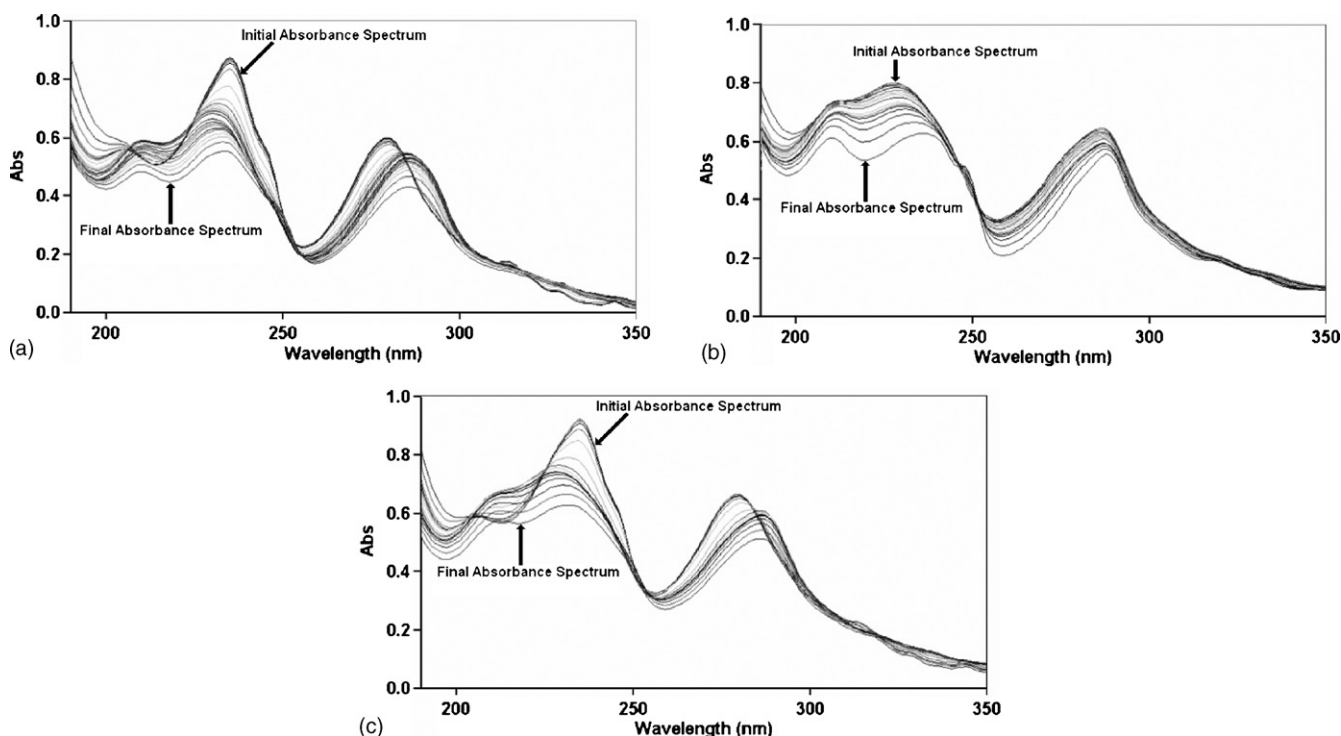


Fig. 12. (a) Spectra of 2×10^{-5} M PDA in 0.1 M NaClO_4 as a function of pH. Initial spectrum is at pH 9.15, while final spectrum is at pH 1.91. (b) Spectra of 2×10^{-5} M PDA with an equimolar amount of Cu(II) as a function of pH. The initial pH is 9.15, and the final pH is 1.91. The spectral changes are due largely to dilution as acid was added. The changes at lowest pH ('final absorbance spectrum') are due to the formation of a Cu(PDAH) complex. (c) Spectra of 2×10^{-5} M PDA with equimolar amounts of Cu(II) and EDTA, as a function of pH in the range 9.15 (initial) to 1.91 (final). At the highest pH values the spectra correspond exactly to those of the free PDA ligand (compare with (a)) at that pH, showing that the Cu(II) is bound by the EDTA. As the pH is lowered, the spectra shift to being those of the Cu(II) complex at the corresponding pH values (compare with (b)). From the variation of absorption here as a function of pH at five different wavelengths the $\log K$ for Eq. (1) can be calculated, which allows for calculation of $\log K_1(\text{PDA})$ for Cu(II) from the known [12] value of $\log K_1(\text{EDTA})$ for Cu(II).

this effect might be even larger for M(IV) ions. This is of considerable potential interest with actinide ions such as U(IV) and Pu(IV), and possibly also the UO_2^{2+} ion. Preliminary work with Th(IV) ($r^+ = 0.96 \text{ \AA}$ [14]) supports the idea that the stabilization

effects of PDA relative to EDDA complexes are dependent on the charge on the metal ion. Thus, competition experiments with DTP A, Th(IV), and PDA [74] suggest $\log K_1(\text{PDA})$ for Th(IV) of about 24, which would represent a 12 log unit stabilization relative to the EDDA complex. This result shows that ligands such as PDA have the potential for achieving remarkable selectivity for M(IV) ions with an ionic radius close to 0.96 \AA . One should note r^+ for U(IV) (0.89) and Pu(IV) (0.86 \AA) [14] as indicating potentially remarkable complexing ability with PDA.

Structures of PDA complexes have been reported [74–78] with Co(II), Ni(II), Mg(II), Cr(III) and Cu(II). These show the consequences of complexation of PDA with these small metal ions. The Ni(II) structure in Fig. 14 shows how with the very small Ni(II) ion, the PDA is only three-coordinating, with one carboxylate group left non-coordinated and H-bonded to a water coordinated to the Ni(II) [75]. Clearly, the problems small metal ions have with coordinating to PDA account for their comparatively low affinity for these ligands. In contrast, the structure of the PDA complex of the large Ca(II) ion in Fig. 15 shows how a metal ion of the appropriate size bonds to all four donor atoms of PDA in a low strain manner, achieving normal Ca–N and Ca–O bonds with all four donor atoms.

The metal ion coordinating properties of PDA point the way to a rich chemistry of complexation of metal ions in solution by the ligands shown in Fig. 11. The complexes of PDA-based ligands with Dy(III) have already found considerable use in biology, with use of modified versions of PDA for docking the

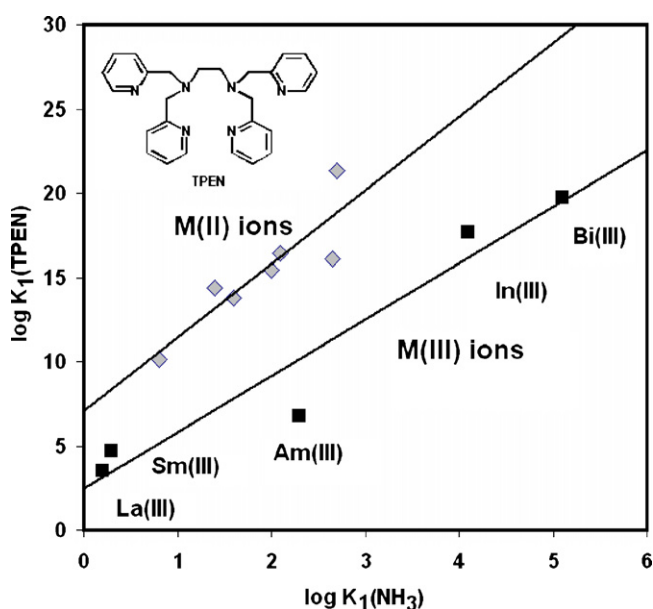


Fig. 13. $\log K_1$ for TPEN complexes [14,72,6] of M(II) and M(III) ions plotted against $\log K_1(\text{NH}_3)$ [8,12] for the same ions.

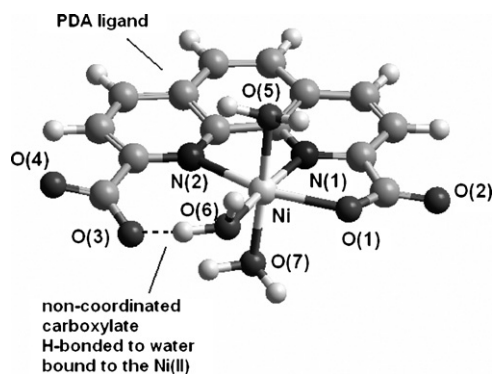


Fig. 14. Ni(II) complex of PDA showing how one carboxylate (O(3)) of PDA is left not coordinated to the Ni(II), but H-bonded to a water molecule (O(6)) coordinated to the Ni(II), which is six-coordinate. Drawing made with Hyperchem [34] using coordinates from ref. [75].

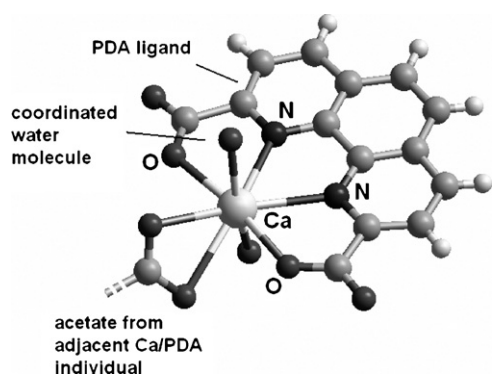


Fig. 15. Structure of the Ca(II) complex of PDA [69].

Dy(III) [79] and Eu(III) [80] complexes in the grooves of DNA. The Eu(III) complex of a sulphonyl substituted PDA has also been used [81] as a fluorescence marker for protein labeling. PDA has also been used in antibody-based assays for the UO_2^{2+} ion [82]. Most of the ligands in Fig. 11 form exclusively five-membered chelate rings on coordination to metal ions, and from the rules relating to chelate ring size and metal-ion selectivity [8], one should expect high selectivity for larger metal ions with r^+ of about 1.0 Å. Some of these ligands, namely, QPHEN, PHP, and DHP in Fig. 11 also will form one or more six-membered chelate rings, which should move selectivity towards smaller metal ions with an ionic radius close to 0.6 Å. The study of these ligands should lead to new insights into factors that control metal-ion recognition by highly preorganized ligands, and ligands of potential usefulness in a wide range of applications [1–4].

Acknowledgment

The authors thank the University of North Carolina Wilmington for generous support for this work.

References

- [1] C. Orvig, M. Abrams, Chem. Rev. 99 (1999) 2201, and following papers in that issue.
- [2] A. Bencini, M.A. Bernardo, A. Bianchi, E. Garcia-Espana, C. Giorgi, S. Luis, F. Pina, B. Valtancoli, Adv. Supramol. Chem. 8 (2002) 79.
- [3] E. Steinhilber, B. Salbu (Eds.), Trace Elements in Natural Waters, CRC Press, Boca Raton, FL, 1995.
- [4] A.E.V. Gorden, J. Xu, K.N. Raymond, Chem. Rev. 103 (2003) 4207.
- [5] D.J. Cram, Science 240 (1988) 76.
- [6] J.M. Lehn, Acc. Chem. Res. 11 (1978) 49.
- [7] C.J. Pederson, J. Am. Chem. Soc. 89 (1967) 2495, 7017.
- [8] R.D. Hancock, A.E. Martell, Chem. Rev. 89 (1989) 1875.
- [9] P. Comba, W. Schiek, Coord. Chem. Rev. 238–239 (2003) 21.
- [10] G.J. Lumetta, B.M. Rapko, P.A. Garza, B.P. Hay, R.D. Gilbertson, T.J.R. Weakley, J.E. Hutchison, J. Am. Chem. Soc. 124 (2002) 5644.
- [11] G. Schwarzenbach, R. Gut, G. Anderegg, Helv. Chim. Acta 37 (1954) 937.
- [12] A.E. Martell, R.M. Smith, Critical Stability Constant Database, 46, National Institute of Science and Technology (NIST), Gaithersburg, MD, USA, 2003.
- [13] A.S. de Sousa, G.J.B. Croft, C.A. Wagner, J.P. Michael, R.D. Hancock, Inorg. Chem. 30 (1991) 3525.
- [14] R.D. Shannon, Acta Crystallogr. A 32 (1976) 751.
- [15] R.D. Hancock, C.J. Siddons, K.A. Oscarson, J.H. Reibenspies, Inorg. Chim. Acta 357 (2004) 723.
- [16] R.D. Hancock, Analyst 122 (1997) 51R.
- [17] R.D. Hancock, A.S. de Sousa, G.B. Walton, J.H. Reibenspies, Inorg. Chem., submitted for publication.
- [18] A.J. Bondi, J. Phys. Chem. 68 (1964) 441.
- [19] R.D. Hancock, J. Chem. Soc., Dalton Trans. (1980) 416.
- [20] V.J. Thorn, J.C.A. Boeyens, G.J. McDougall, R.D. Hancock, J. Am. Chem. Soc. 106 (1984) 3198.
- [21] R.D. Hancock, M.P. Ngwenya, P.W. Wade, J.C.A. Boeyens, S.M. Dobson, Inorg. Chim. Acta 164 (1989) 73.
- [22] K. Damu, H. Maumela, R.D. Hancock, J.C.A. Boeyens, S.M. Dobson, J. Chem. Soc., Dalton Trans. (1991) 2717.
- [23] R.D. Hancock, in: S.R. Cooper (Ed.), Crown Compounds, Towards Future Applications, VCH Publishers, Deerfield Creek, 1992, p. 167.
- [24] R.D. Hancock, G. Patrick, G.D. Hosken, Pure Appl. Chem. 65 (1993) 473.
- [25] E.J. Billo, Inorg. Nucl. Chem. Lett. 11 (1975) 491.
- [26] K. Kanamori, W.E. Broderick, R.F. Jordan, R.D. Willett, J.I. Legg, J. Am. Chem. Soc. 108 (1986) 7122.
- [27] M. Du, X.-H. Bu, J. Mol. Struct. 692 (2004) 195.
- [28] R.D. Hancock, M.P. Ngwenya, A. Evers, P.W. Wade, J.C.A. Boeyens, S.M. Dobson, Inorg. Chem. 29 (1990) 264.
- [29] M.V. Rampersand, S.P. Jeffrey, J.H. Reibenspies, C.G. Ortiz, D.J. Darensbourg, M.Y. Darensbourg, Angew. Chem., Int. Ed. 44 (2005) 1217.
- [30] K. Wright-Garcia, J. Basinger, S. Williams, C. Hu, P.S. Wagenknecht, L.C. Nathan, Inorg. Chem. 42 (2003) 4885.
- [31] Cambridge Crystallographic Data Centre, 12 Union Road, Cambridge CB2 1EZ, United Kingdom.
- [32] D.K. Mills, J.H. Reibenspies, M.Y. Darensbourg, Inorg. Chem. 29 (1990) 4364.
- [33] P.J. Farmer, J.H. Reibenspies, P.A. Lindahl, M.Y. Darensbourg, J. Am. Chem. Soc. 115 (1993) 4665.
- [34] Hyperchem program, Version 7.5, Hypercube, Inc., 419 Philip Street, Waterloo, Ontario N2L 3X2, Canada.
- [35] H. Stetter, K. Dieminger, Chem. Ber. 92 (1959) 2658.
- [36] (a) G.D. Hosken, R.D. Hancock, J. Chem. Soc., Chem. Commun. (1994) 1363; (b) G.D. Hosken, C.C. Allan, J.C.A. Boeyens, R.D. Hancock, J. Chem. Soc., Dalton Trans. (1995) 3705.
- [37] C. Bleiholder, H. Boerzel, P. Comba, R. Ferrari, H. Rosana, M. Heydt, M. Kerscher, S. Kuwata, L. Shigemasa, G. Laurenczy, G.A. Lawrance, A. Lienke, B. Martin, M. Merz, B. Nuber, H. Pritzkow, Inorg. Chem. 44 (2005) 8145.
- [38] H. Boerzel, P. Comba, K.S. Hagen, Y.D. Lampeka, A. Lienke, G. Linti, M. Merz, H. Pritzkow, L.V. Tsymbal, Inorg. Chim. Acta 337 (2002) 407.
- [39] P. Comba, M. Kerscher, A. Roodt, Eur. J. Inorg. Chem. (2004) 4640.
- [40] S.J. Vatsadze, V.S. Tyurin, N.V. Zyk, A.V. Chukarov, L.G. Kuz'mina, E.V. Avtomonov, R.D. Rakhimov, K.P. Butin, Russ. Chem. Bull. Int. Edn. 54 (2005) 1825.

- [41] M.R. Bukowski, P. Comba, A. Lienke, C. Limberg, C. Lopez de Laorden, R. Mas-Balleste, M. Merz, L. Que Jr., *Angew. Chem., Intl. Edn.* 45 (2006) 3446.
- [42] Y. Miyahara, K. Goto, T. Inazu, *Tetrahedron Lett.* 42 (2001) 3097.
- [43] P. Comba, H. Pritzkow, W. Schiek, *Angew. Chem., Intl. Edn.* 40 (2001) 2465.
- [44] C.J. Chandler, L.W. Deady, J.A. Reiss, *J. Heterocycl. Chem.* 18 (1981) 599.
- [45] Y.-Z. Hu, M.H. Wilson, R. Zong, C. Bonnefous, D.R. McMillin, R.P. Thummel, *Dalton Trans.* (2005) 354.
- [46] R.A. Berthon, S.B. Colbran, D.C. Craig, *Polyhedron* 11 (1992) 243.
- [47] B.M. Holligan, J.C. Jeffrey, M.D. Ward, *J. Chem. Soc., Dalton Trans.* (1992) 3337.
- [48] S.-N. Pun, W.-H. Chung, K.M. Lam, P. Guo, P.-H. Chan, K.-Y. Wong, C.-M. Che, T.-Y. Chen, S.-M. Peng, *J. Chem. Soc., Dalton Trans.* (2002) 575.
- [49] J. Cody, J. Dennison, J. Gilmore, D.G. VanDerveer, M.M. Henary, A. Gabrielli, C.D. Sherrill, Y. Zhang, C.-P. Pan, C. Burda, C.J. Fahrni, *Inorg. Chem.* 42 (2003) 4918.
- [50] J.C. Jeffrey, P. Thornton, M.D. Ward, *Inorg. Chem.* 33 (1994) 3612.
- [51] J.-P. Collin, P. Gavina, J.-P. Sauvage, A. De Cian, J. Fischer, *Aust. J. Chem.* 50 (1997) 951.
- [52] Y.-Y. Lin, S.C. Chan, M.C.W. Chan, Y.-J. Hou, N. Zhou, C.-M. Che, Y. Liu, Y. Wang, *Chem. Eur. J.* 9 (2003) 1263.
- [53] D.A. Bardwell, A.M.W. Cargill Thompson, J.C. Jeffrey, E.E.M. Tilley, M.D. Ward, *J. Chem. Soc., Dalton Trans.* (1995) 835.
- [54] R.J.M. Gebbink, M. Watanabe, R.C. Pratt, T.D.P. Stack, *Chem. Commun.* (2003) 630.
- [55] Y. Bretonniere, R. Wietzke, C. Lebrun, M. Mazzanti, J. Pecaut, *Inorg. Chem.* 39 (2000) 3499.
- [56] C. Bazzicalupi, A. Bencini, E. Berni, A. Bianchi, L. Borsari, C. Giorgi, B. Valtancoli, C. Lodeiro, J.C. Lima, A.J. Parola, F. Pina, *Dalton Trans.* (2004) 591.
- [57] T.F. Liu, H.K. Lin, S.R. Zhu, Z.M. Wang, H.G. Wang, X.B. Leng, Y.T. Chen, *J. Mol. Struct.* 597 (2001) 199.
- [58] C. Bazzicalupi, A. Bencini, S. Ciattini, C. Giorgi, A. Masotti, P. Paoletti, B. Valtancoli, N. Navon, D. Meyerstein, *J. Chem. Soc., Dalton Trans.* (2000) 2383.
- [59] A. Angeloff, J.-C. Daran, J. Bernadou, B. Meunier, *Eur. J. Inorg. Chem.* (2000) 1985.
- [60] J.G.P. Delis, M. Rep, R.E. Rulke, P.W.N.M. Van Leeuwen, K. Vriese, J. Fraanje, K. Goubitz, *Inorg. Chim. Acta* 250 (1996) 87.
- [61] M. Carcelli, S. Janelli, P. Pelagatti, G. Pelizzi, D. Rogolina, C. Solinas, M. Tegoni, *Inorg. Chim. Acta* 358 (2005) 903.
- [62] S. Toyota, A. Goto, K. Kaneko, T. Umetani, *Heterocycles* 65 (2005) 551.
- [63] C.R. Rice, K.M. Anderson, *Polyhedron* 19 (2000) 495.
- [64] Md.A. Masood, D.J. Hodgson, *Inorg. Chem.* 32 (1993) 4839.
- [65] C.-M. Liu, S. Gao, H.-Z. Kou, *Chem. Commun.* (2001) 1670.
- [66] K.H. Sugiyarto, D.C. Craig, H.A. Goodwin, *Aust. J. Chem.* 49 (1996) 497.
- [67] H. Aghabazorg, C.J. Palenik, R.C. Palenik, *J. Sci. I.R. Iran* 2 (1991) 103.
- [68] R. Zong, R.P. Thummel, *J. Am. Chem. Soc.* 126 (2004) 10800.
- [69] D.L. Melton, D.G. VanDerveer, R.D. Hancock, *Inorg. Chem.* 45 (2006) 9306.
- [70] R.M. Dyson, G.A. Lawrance, H. Macke, M. Maeder, *Polyhedron* 18 (1999) 3243.
- [71] R.D. Hancock, *Acc. Chem. Res.* 26 (1990) 875.
- [72] J.M. Harrington, K.A. Oscarson, S.B. Jones, J.H. Reibenspies, L.J. Bartolotti, R.D. Hancock, *Zeit. Naturforsch. B*, in press.
- [73] M.P. Jensen, L.R. Morss, J.V. Beitz, D.D. Ensor, *Alloys Compd.* 303–304 (2000) 137.
- [74] A. Moghimi, R. Alizadeh, A. Shokrallaki, H. Aghabazorg, M. Shamsipur, A. Shokravi, *Inorg. Chem.* 42 (2003) 1616.
- [75] Y.-B. Xie, J.-R. Li, X.-H. Bu, *J. Mol. Struct.* 741 (2005) 249.
- [76] K.M. Park, I. Yoon, J. Seo, Y.H. Lee, S.S. Lee, *Acta Crystallogr., Sect. E: Struct. [Reports Online]* 57 (2001) m154.
- [77] A. Moghimi, R. Alizideh, M.C. Aragoni, V. Lippolis, H. Aghabazorg, P. Norouzi, F. Isaia, S. Sheshmani, *Anorg. Allg. Chem.* 631 (2005) 1941.
- [78] A. Moghimi, R. Alizideh, H. Aghabazorg, A. Shokravi, M.C. Aragoni, F. Demartin, F. Isaia, V. Lippolis, A. Harrison, A. Shokrollahi, M. Shamsipur, *J. Mol. Struct.* 750 (2005) 166.
- [79] J. Coates, P.G. Sammes, R.M. West, *J. Chem. Soc., Perkin Trans. 2* (7) (1996) 1275.
- [80] E.P. Diamandis, R.C. Morton, *J. Immunol. Meth.* 112 (1988) 43.
- [81] S.T. Mullins, P.G. Sammes, R.M. West, G. Yahiloglu, *J. Chem. Soc., Perkin Trans. 1* (1996) 75.
- [82] D.A. Blake, A.R. Pavlov, H. Yu, M. Kohsravi, H.E. Ensley, R.C. Blake II., *Anal. Chim. Acta* 444 (2001) 3.